



Proceeding Paper

# Towards Transformative Healthcare Applications: Biomimetic Hydroxyapatite Systems for Controlled Drug Delivery †

Olumakinde Omiyale

 $In fochemistry\ Scientific\ Centre,\ ITMO\ University,\ Saint\ Petersburg\ 197101,\ Russia;\ oomii ale@itmo.ru$ 

† Presented at the 29th International Electronic Conference on Synthetic Organic Chemistry (ECSOC-29); Available online: https://sciforum.net/event/ecsoc-29.

#### **Abstract**

Recently, there has been a growing interest in multifunctional materials, therefore we developed a system that combines biocompatibility, gradient changing and antibacterial properties. We aim to combine these properties in the development of a biomimetic system based on hydroxyapatite (Ca10(PO4)6(OH)2, HA) by incorporating silver nanoparticles (Ag NPs) into HA matrices, leveraging their antimicrobial effects, while also exploring their role as drug release triggers (absorb infrared (IR) light of 808-960 nm, convert to heat energy to induce localized heating and cause a structure leak for drug release) to unmodified HA which cannot be activated by IR in significant amounts. Limited diffusion aggregation is used to form HA (enhanced with glycine or produced with different outer electrolytes) by diffusing calcium phosphates through Na2HPO4-agar. The composite was then packed with tetracycline and deposition of polyelectrolytes (PE). The combination of polydiallyldimethylammonium chloride (PDADMAC) and heparin forms a robust PE. Infrared light (808 nm, 1.4 mW/cm<sup>2</sup>) was utilized as energy source for non-invasive and ondemand drug release. Physical and chemical characterization of HA was carried out. Glycine did not affect the p-factor of the resulting rings, which is equal to ca. 1.00. NIR increased release rates 2.1-fold (k = 39.21 compared to 18.22). High glycine concentrations reduces HA crystallinity (94 to 30%), a 12.5% increased drug loading capacity, increases solubility (5× control). NIR reduced the Korsmeyer-Peppas release exponent (n) from 0.42 (Fickian) to 0.11 (PE-coated HA-Ag), confirming photothermal disruption of diffusion barriers due to the presence of silver nanoparticle peaks in the composition.

Keywords: hydroxyapatite patterns; infrared-triggered release; tetracycline

Academic Editor(s): Name

Published: date

Citation: Omiyale, O. Towards Transformative Healthcare Applications: Biomimetic Hydroxyapatite Systems for Controlled Drug Delivery. *Chem. Proc.* **2025**, *volume number*, x. https://doi.org/10.3390/xxxxx

Copyright: © 2025 by the author. Submitted for possible open access publication under the terms and conditions of the Creative Commons Attribution (CC BY) license (https://creativecommons.org/license s/by/4.0/).

### 1. Introduction

This research is devoted to the development of a biomimetic system based on hydroxyapatite (Ca<sub>10</sub>(PO<sub>4</sub>)<sub>6</sub>(OH)<sub>2</sub>, HA), modified by amino acids, silver nanoparticles and infrared-sensitive polyelectrolytes (PE) to prolong drug release. Beyond its structural role, HA's multifunctionality confers the essential characteristics required for use as a local drug delivery biocompatible coating. This is owing to its near resemblance in composition and structure to the primary inorganic component of bones. Nowadays, there has been a growing interest in multifunctional materials, therefore we have decided to present a system that combines biocompatibility, gradient changing and antibacterial properties. In this study, we aim to combine these properties by incorporating silver nanoparticles (Ag NPs) into HA matrices, leveraging their well-documented antimicrobial effects, while also

Chem. Proc. 2025, x, x https://doi.org/10.3390/xxxxx

exploring their role as drug release triggers to unmodified/pure HA which cannot be activated by IR in significant amounts without this functionalization. The Ag NPs are known to absorb the IR light of 808–960 nm depending on their size (40–100 nm in diameter) and convert it into heat energy which can induce localized heating and cause a structure leak or increase the permeability of the matrix which consequently leads to release of the packed drugs [1,2].

# 2. Materials and Methods

Calcium nitrate tetrahydrate (Ca(NO<sub>3</sub>)<sub>2</sub>·4H<sub>2</sub>O, 99% purity), disodium hydrogen phosphate (Na<sub>2</sub>HPO<sub>4</sub>), sodium hydroxide (NaOH), and glycine bought from Sigma Aldrich. Hydrochloric acid (HCl, 37%), polydiallyldimethylammonium chloride (PDADMAC) solution (20% *w/v* concentration: 1 mg/mL), Heparin sodium salt solution (concentration: 5000 EU). The system involves agar diffusion, resulting in the formation of HA (enhanced with glycine of different concentrations or produced with different outer electrolytes) through the diffusion of calcium phosphates through Na<sub>2</sub>HPO<sub>4</sub>. The composite was then incorporated with tetracycline hydrochloride and deposition of PE [3]. The combination of polydiallyldimethylammonium chloride (PDADMAC) and heparin forms a robust PE, while HA provides a biocompatible matrix. Infrared (IR) light at (808 nm, 1.4 mW/cm<sup>2</sup>) was utilized as a trigger for controlled drug release, offering a non-invasive method to modulate therapeutic delivery.

Physical and chemical characterization of HA was carried out. Infrared spectra were scanned with Nicolet iS5 FTIR Spectrometer (Nicolet Instrument Corporation, WI, USA). Scanning electron microscopy Quanta inspect S microscope (FEI Company Scanning Electron Microscope, USA) was used to study the morphology and size of the samples. Electron Dispersive Xray Spectroscopy (EDX) EDXA equipment with dispersive Xray was used to confirm powder sample composition and identify phase peaks. The X-ray diffraction (XRD) was used to analyze the crystalline structure phase, purity and crystallinity of the HA powders and zeta potential measurements of all samples was determined in water before and after loading with tetracycline at room temperature (25 °C). Photocor Compact Z Zetasizer (Moscow, Russia).

Drug Release Kinetics Zero-order kinetics model. Equation (1)

$$t = C_0 + k_0 t \tag{1}$$

Ct is the concentration of the drug remaining at time t,  $C_0$  is the initial concentration of the drug, and  $K_0$  is the zero-order rate constant.

First-order kinetics model. Equation (2)

$$\log Ct = \log Co - (k_1 t)/2.303$$
 (2)

K1 is the first-order rate constant.

Korsmeyer-Peppas kinetics model. Equation (3)

$$Mt/M\alpha = ktn$$
 (3)

 $Mt/M\alpha$  is the fraction of the drug released at time t, k is the rate constant, and n is the release exponent indicating the drug transport mechanism through the polymer [4].

# 3. Results and Discussion

The different concentrations of glycine are found to have a significant effect on the crystallinity of the HA due to its effect on kinetic of HA crystallization (nucleation of new crystals) by enhancing the surface diffusion mechanism in the precipitate. It was found that the addition of glycine to the system does not affect the p-factor of the resulting rings, which is equal to ca. to 1.00. NIR increased release rates 2.1-fold (k = 39.21 compared to

18.22). High glycine concentrations reduces HA crystallinity (94 to 30%), a 12.5% increased drug loading capacity, increases solubility ( $5 \times$  control). Furthermore, in the silver nanoparticles infused composites, the NIR light reduced the Korsmeyer-Peppas release exponent (n) from 0.42 (Fickian) to 0.11 (PE-coated HA-Ag), confirming photothermal disruption of diffusion barriers due to the presence of silver nanoparticle peaks in the composition (Figure 1).

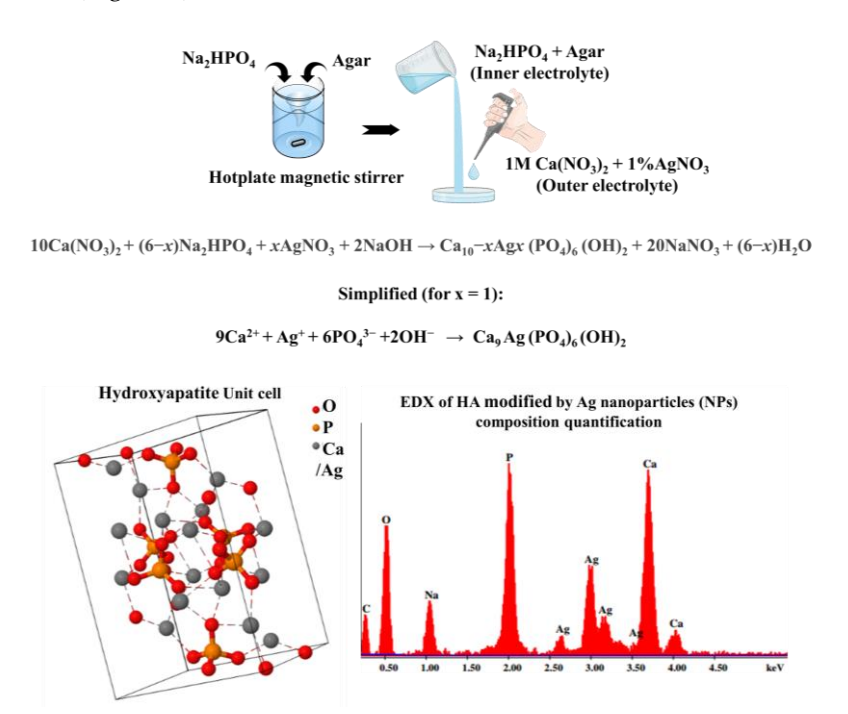


**Figure 1.** Research plan. Limited Diffusion Aggregation where outer electrolyte, 1 M CaCl<sub>2</sub> (control), 1 M Ca(NO)<sub>3</sub>, or a combination of 1 weight percent AgNO<sub>3</sub> and Ca(NO)<sub>3</sub> was diffused into an inner electrolyte solution that contained agar and 0.2M Na<sub>2</sub>HPO<sub>4</sub>.

#### 3.1. Hydroxyapatite Characterization

Scanning electron microscopy (SEM) showed irregular particle shapes in glycine-modified hydroxyapatite (HA) composites, with glycine concentration significantly influencing particle size. Unmodified HA (0 mg/mL glycine) showed the smallest average particle size (55.6 nm), reflecting higher crystallinity (as corroborated by XRD). Glycine-modified HA exhibits progressive reduction in average particle size with increasing glycine concentration—94.3 nm (0.5 mg/mL), 89.3 nm (1 mg/mL), and 75.5 nm (2 mg/mL). Glycine inhibits crystal growth and promotes nanostructuring. The study found glycine-enhanced and pure hydroxyapatite have nearly identical p-factor values, indicating glycine's effects on HA properties may not translate into significant differences. This explains higher drug loading and potential bone-targeted applications.

The Ca/P ratios of pure HA (1.41) deviated from stoichiometric HA (1.67), with lower ratios indicating non-stoichiometric or defective structures. The defective, non-stoichiometric, observed HA Ca/P ratio (for 1–2 mg/mL glycine modified HA ranged between 1.32–1.14). Glycine's interaction with HA led to a 3.6-fold increase in HA solubility at 2 mg/mL glycine compared to 0.5 mg/mL. This suggests that glycine disrupts the HA Lattice, leading to defects and improved drug adsorption. Defective, non-stoichiometric HA has more surface vacancies and functional groups, improving drug adsorption due to factors such as changes in crystal structure, particle size and surface properties of HA.

The micrographs for the powders that were obtained from the HA rings formed with different outer electrolytes of 1 M CaCl<sub>2</sub>, 1 M Ca(NO<sub>3</sub>)<sub>2</sub>, a mixture of 1 M Ca(NO<sub>3</sub>)<sub>2</sub> and 1

wt. % AgNO<sub>3</sub>. display fine-grained nanostructures and a uniform distribution. According to prior research, this particular form is typical of hydroxyapatite produced by the agar diffusion process. [5] The crystallinity trends (HA from CaCl<sub>2</sub> electrolyte exhibited 90% crystallinity, HA produced with only 1 M Ca(NO<sub>3</sub>)<sub>2</sub> showed 65% crystallinity while HA produced with a mixture of 1M Ca(NO<sub>3</sub>)<sub>2</sub> and 1wt. % AgNO<sub>3</sub> as electrolyte showed 59% crystallinity), as observed by [6], were correlated with the irregularly shaped HA particle diameters of ca. 55.6 nm (HA-Cl), 86.8 nm (HA-Ca(NO<sub>3</sub>)<sub>2</sub>), and 80.8 nm (HA-Ag) as determined by SEM. The particle size and morphology variations reflect the influence of electrolyte composition on HA formation and silver doping [7].

Electron Dispersive Xray Spectroscopy (EDX) has identified the elemental composition and phases of hydroxyapatite (HA) samples, with a mixture of 1 M Ca(NO<sub>3</sub>)<sub>2</sub> and 1 wt.% AgNO<sub>3</sub> producing silver peaks. The HA-Ag composite showed 12.4 wt.% Ag incorporation, similar to previous studies on antibacterial efficacy. The samples were consistent with hydroxyapatite and were found to be composed of elongated nanocrystallites. XRD analysis of HA-Ag powders revealed good crystal structure and apatite properties, making it suitable for controlled drug delivery and antibacterial coatings. The study also revealed that the surface charge of particles in colloidal systems affects their stability and interaction. HA-Cl, a CaCl<sub>2</sub>-based HA, shows moderate stability before and after drug loading of tetracycline into composites. Silver-modified HA, HA-Ag, shows a significant increase in negativity after TET loading, indicating synergistic interactions (Figure 1).

# 3.2. In Vitro Tetracycline Drug Loading and IR Controlled Drug Release

# 3.2.1. Drug Loading Efficiency

The UV-Vis spectrophotometry analysis revealed that drug loading efficiency varied with glycine concentration. Higher concentrations improved drug loading by 12.5%, likely due to increased surface porosity and carboxylate-drug interactions. Films with 0.5 mg/mL glycine exhibited the lowest loading efficiency, likely due to the interaction between glycine and hydroxyapatite eroding binding sites for tetracycline. Glycine 1 and 2 mg/mL showed better loading than 0.5 mg/mL glycine, suggesting increased porosity may have aided with packing hydroxyapatite and subsequently interacting better with drug molecules. Glycine can create more functional groups on the hydroxyapatite surface, which can interact with drug molecules through hydrogen bonding, electrostatic interactions, or van der Waals forces, improving drug loading efficiency [8]. Films prepared with different electrolytes showed varying drug loading properties, the mixture of 1 M Ca(NO<sub>3</sub>)<sub>2</sub> and 1 wt. % AgNO<sub>3</sub> yielded samples that loaded more drugs (0.30 ± 0.03 mg), than control, CaCl<sub>2</sub> at 0.21 ± 0.02 mg despite higher crystallinity (90%).

# 3.2.2. Drug Release

Experimental conditions accelerating release such as infrared (IR) light (808 nm, 1.4 mW/cm²) disrupts electrostatic/drug bonds, causing photothermal burst release. This artificially inflates initial rates, shortening apparent  $t\frac{1}{2}$ . For example, NIR increased release rates 2.1-fold (k = 39.21 compared to 18.22). High glycine concentrations reduces HA crystallinity (94% to 30%) and increases solubility (5× control), creating porous matrices that accelerate diffusion. At 1–2 mg/mL glycine, faster release aligns with smaller particle sizes (75.5–89.3 nm, SEM data) and also uncoated HA samples without polyelectrolyte (PE) coatings showed 78.6% release in 1 h), as no diffusion barrier exists.

The study found that IR light effectively triggered the release of tetracycline from films, with rapid release followed by a prolonged liberation phase. HA samples with different electrolytes released more drugs under NIR triggering, confirming Ag NPs' ability to enable photothermal-triggered release. HA Sample powders from a mixture of

 $1 \text{ M Ca}(NO_3)_2$  and  $1 \text{ wt. } \% \text{ AgNO}_3$  as electrolyte released tetracycline (0.06 mg/mL at 400 min) 4 times faster than CaCl<sub>2</sub> (0.02 mg/mL at 400 min) and Ca(NO<sub>3</sub>)<sub>2</sub>. (0.02 mg/mL at 400 min). The 4-fold increase in drug release from HA-Ag under NIR confirms the hypothesis that Ag NPs enable photothermal-triggered release by converting NIR to localized heat [9].

## 3.2.3. Kinetics Analysis

The overall interpretation of the study suggests that the presence of NIR (808 nm, 1.4 mW/cm²) tends to result in faster release rates disrupts electrostatic/drug bonds, causing photothermal burst release and potentially more complex release mechanisms. (Figure 2A) This artificially inflates initial rates, shortening apparent  $t^{1/2}$ . For example, NIR increased release rates 2.1-fold (k = 39.21 compared to 18.22). High glycine concentrations reduces HA crystallinity (94% to 30%) and increases solubility (5× control), creating porous matrices that accelerate diffusion. At 1–2 mg/mL glycine, faster release aligns with smaller particle sizes (75.5–89.3 nm, SEM data) and also uncoated HA samples without polyelectrolyte (PE) coatings showed 78.6% release in 1 h, as no diffusion barrier exists.

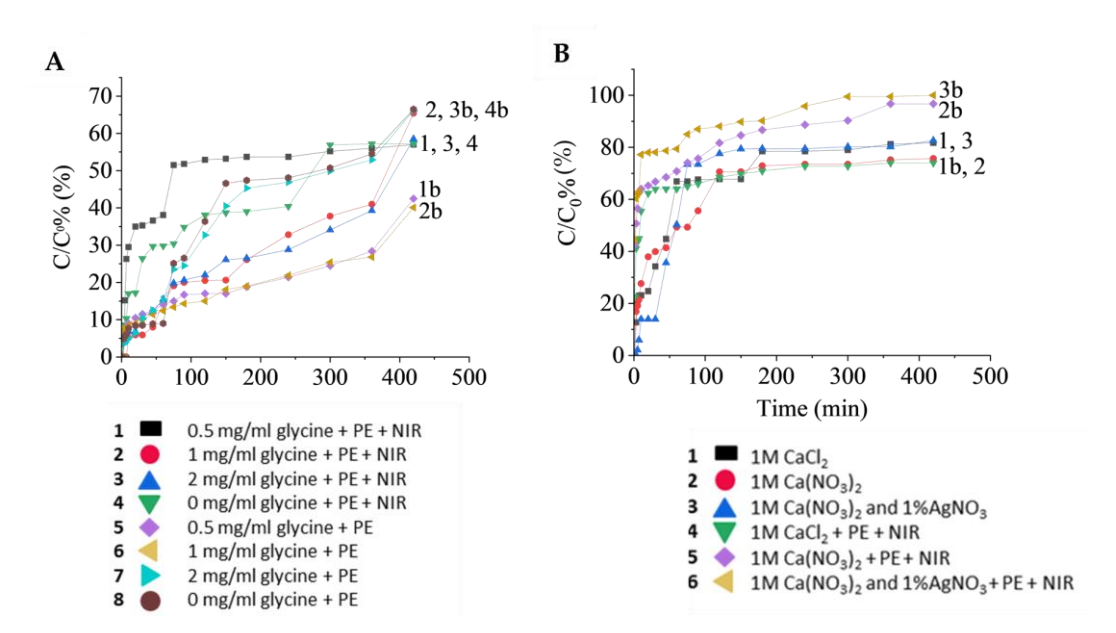


**Figure 2.** Drug release profiles of HA powder samples (obtained using CaCl<sub>2</sub>: plot 1), HA (obtained using Ca(NO<sub>3</sub>)<sub>2</sub>: plot 2), and HA modified by Ag nanoparticles (NPs): plot 3, and/or encapsulated with 0.125M PDADMAC/0.125M heparin and/or assisting with NIR. (**A**) HA samples coated with PDADMAC/Heparin PE and assisted with NIR (plot 1–3) as compared with PDADMAC/Heparin PE only (plot 1b–3b). (**B**) HA-GLY samples coated with PDADMAC/Heparin PE and assisted with NIR (plot 1–4) as compared with PDADMAC/Heparin (plot 1b–4b).

The primary release mechanism (identified as Fickian diffusion, swelling, or erosion) using the Korsmeyer-Peppas model and the release exponent (n). The composite system involves glycine-induced porosity (SEM), PE coatings (diffusion barriers) and NIR-triggered disruption (photothermal effects). The results reveal that uncoated HA showed Fickian diffusion (n < 0.45), where release is pore mediated. PE-coated HA showed non-Fickian (n = 0.66–0.81), suggesting combined diffusion/polymer relaxation.

The release mechanism of a material is affected by the presence of different electrolytes (1 M CaCl<sub>2</sub>, 1 M Ca(NO<sub>3</sub>)<sub>2</sub>, a mixture of 1 M Ca(NO<sub>3</sub>)<sub>2</sub> and 1 wt. % AgNO<sub>3</sub>). Fickian diffusion is the most common, with HA-Ag showing slower release rates without PE coating (Figure 2B). The Fickian diffusion mechanism (n = 0.42) aligns with [10], who observed similar kinetics in mesoporous HA. The heparin/PDADMAC PE coating

reduced the release rate constant (k) from 0.04 h<sup>-1</sup> to 0.001 h<sup>-1</sup>). Ref. [11] found similar results for coatings made of calcium phosphate that are modified with iron and have antibacterial qualities.

The following key findings on electrolyte-dependent structural properties, p-factor and Liesegang ring formation show that HA-Cl (CaCl<sub>2</sub>) and HA-Ca(NO<sub>3</sub>)<sub>2</sub> exhibited p-factors  $\approx 1.00$ , indicating regular ring spacing and homogeneous nucleation. Electrolyte impact on Ca/P ratios shows HA-Cl (1.41), HA-Ca(NO<sub>3</sub>)<sub>2</sub> (1.97) and HA-Ag (0.97), where Ag+ substitution created Ca-deficient HA, disrupting nucleation in the HA lattice. The crystallinity and phase content of HA-Cl revealed it has the highest crystallinity (90%) with minimal defects, favoring rapid drug diffusion. HA-Ca(NO<sub>3</sub>)<sub>2</sub> had lower crystallinity (65%) and higher porosity, enhancing drug adsorption and HA-Ag recorded intermediate crystallinity (59%) with 12.4 wt. % Ag, confirmed by EDX, introducing defects but improving photothermal response. Korsmeyer-Peppas best fit all samples, showing Fickian diffusion ( $n \approx 0.3$ –0.4), with R<sup>2</sup> > 0.92. NIR reduced n to 0.11 for PE-coated HA-Ag, confirming photothermal disruption.

Future directions include optimization of Ag loading to balance antibacterial efficacy with release kinetics. In vivo validation tests on PE-coated HA-Ag in bone defect models and advanced modeling using Density Functional Theory simulations to predict drug-HA binding energies

# 4. Conclusions

The findings indicated that varying glycine amino acid concentrations had a number of important effects on the system, including on the hydroxyapatite's crystallinity because they improved the precipitate's surface diffusion mechanism and influenced the kinetics of hydroxyapatite crystallization, or the formation of new crystals.

This work demonstrates that electrolyte choice,  $Ca(NO_3)_2$  or Ag modification critically tune HA's structure, drug affinity, and release profiles. The  $Ca(NO_3)_2 + 1$  wt. % AgNO<sub>3</sub> system (p-factor = 0.81) emerges as the most versatile, offering: high drug loading (HA-Ag loaded 52% more tetracycline than HA-Cl,  $0.30 \pm 0.03$  mg), photothermal responsiveness (4× faster release under NIR) and PE-compatible sustained release.

These findings could pave the way for smart, multifunctional HA coatings in orthopedics, dentistry, and targeted therapy. The study finds applications in biomedicine such as bone implant coatings, and HA-Ag assisted with NIR for on-demand infection control  $(t_1/2 = 2.57 \text{ h})$  under irradiation). As wound dressings, PE-coated HA-Ag combines sustained antimicrobial action (Ag<sup>+</sup>) with triggerable drug release. In cancer therapy, NIR-responsive HA-Ag could deliver chemotherapeutics locally with spatiotemporal control. Glycine addition to hydroxyapatite enhances even bioactivity, and compatibility with bone tissue, making it a promising candidate for regenerative medicine and bone repair strategies, providing insights for optimizing biomaterials.

**Funding:** This research received no external funding.

**Institutional Review Board Statement:** Not applicable.

Informed Consent Statement: Not applicable.

Data Availability Statement: Available on request.

**Acknowledgments:** Great appreciation to Svetlana Ulasevich and Ekaterina Skorb for guidance on the project.

Conflicts of Interest: The authors declare no conflicts of interest.

# **Abbreviations**

The following abbreviations are used in this manuscript:

PDADMAC Polydiallyldimethylammonium chloride

HA Hydroxyapatite
PE Polyelectrolyte
AgNPs Silver nanoparticles
TET Tetracycline

NIR Near Infrared Radiation CDR Cumulative Drug Release R<sup>2</sup> Correlation coefficient

### References

- Kubiak-Mikkelson, Z.; Kostrzębska, A.; Błaszczyszyn, A.; Pitułaj, A.; Dominiak, M.; Gedrange, T.; Nawrot-Hadzik, I.; Matys, J.; Hadzik, J. Ionic Doping of Hydroxyapatite for Bone Regeneration: Advances in Structure and Properties over Two Decades — A Narrative Review. Appl. Sci. 2025, 15, 1108. https://doi.org/10.3390/app15031108.
- 2. Omiyale, O.C.; Musa, M.; Otuyalo, A.I.; Gbayisomore, T.J.; Onikeku, D.Z.; George, S.D.; Popoola, P.O.; Olofin, O.O.; Umunnam, K.F.; Nneji, P.O.; Adnan, M. A Review on Selenium and Gold Nanoparticles Combined Photodynamic and Photothermal Prostate Cancer Tumors Ablation. *Discov. Nano* 2023, *18*, 150. https://doi.org/10.1186/s11671-023-03936-z.
- 3. Mysore, T.H.M.; Patil, A.Y.; Hegde, C.; Sudeept, M.A.; Kumar, R.; Soudagar, M.E.M.; Fattah, I.M.R. Apatite Insights: From Synthesis to Biomedical Applications. *Eur. Polym. J.* **2024**, 209, 112842. https://doi.org/10.1016/j.eurpolymj.2024.112842.
- 4. Angan, A.; Sambudi, N.S. Synthesis of Alginate/Hydroxyapatite Beads for Acetaminophen Delivery. *Makara J. Sci.* **2022**, *26*, 4. https://doi.org/10.7454/mss.v26i3.1385.
- 5. Eltantawy, M.M.; Belokon, M.A.; Belogub, E.V.; Ledovich, O.I.; Skorb, E.V.; Ulasevich, S.A. Self-Assembled Liesegang Rings of Hydroxyapatite for Cell Culturing. *Adv. NanoBiomed Res.* **2021**, *1*, 2000048. https://doi.org/10.1002/anbr.202000048.
- 6. Matsumoto, T.; Okazaki, M.; Inoue, M.; Hamada, Y.; Taira, M.; Takahashi, J. Crystallinity and Solubility Characteristics of Hydroxyapatite Adsorbed Amino Acid. *Biomaterials* **2002**, 23, 2241–2247. https://doi.org/10.1016/S0142-9612(01)00358-1.
- 7. Zhao, X.Y.; Zhu, Y.J.; Chen, F.; Lu, B.Q.; Qi, C.; Zhao, J.; Wu, J. Calcium Phosphate Hybrid Nanoparticles: Self-Assembly Formation, Characterization, and Application as an Anticancer Drug Nanocarrier. *Chem. Asian J.* **2013**, *8*, 1306–1312. https://doi.org/10.1002/asia.201300083.
- 8. Rusu, L.C.; Nedelcu, I.A.; Albu, M.G.; Sonmez, M.; Voicu, G.; Radulescu, M.; Sinescu, C. Tetracycline Loaded Collagen/Hydrox-yapatite Composite Materials for Biomedical Applications. *J. Nanomater.* **2015**, 2015, 361969. https://doi.org/10.1155/2015/361969.
- Ciobanu, C.S.; Iconaru, S.L.; Chifiriuc, M.C.; Costescu, A.; Le Coustumer, P.; Predoi, D. Synthesis and Antimicrobial Activity of Silver-Doped Hydroxyapatite Nanoparticles. *BioMed Res. Int.* 2013, 2013, 916218. https://doi.org/10.1155/2013/916218.
- 10. Fosca, M.; Streza, A.; Antoniac, I.V.; Vadalà, G.; Rau, J.V. Ion-Doped Calcium Phosphate-Based Coatings with Antibacterial Properties. *J. Funct. Biomater.* **2023**, *14*, 250. https://doi.org/10.3390/jfb14050250.

**Disclaimer/Publisher's Note:** The statements, opinions and data contained in all publications are solely those of the individual author(s) and contributor(s) and not of MDPI and/or the editor(s). MDPI and/or the editor(s) disclaim responsibility for any injury to people or property resulting from any ideas, methods, instructions or products referred to in the content.